

# IRS spectroscopic studies of ULIRGs at $z \sim 2$

Guanwen Fang<sup>1</sup>, Xu Kong<sup>2,3</sup>, Jia-Sheng Huang<sup>4</sup> and Zhongyang Ma<sup>2</sup>

<sup>1</sup>Institute for Astronomy and History of Science and Technology, Dali University, Yunnan, 671003, China

<sup>2</sup>Center for Astrophysics, University of Science and Technology of China, Anhui, 230026, China  
email: xkong@ustc.edu.cn

<sup>3</sup>Key Laboratory for Research in Galaxies and Cosmology, Chinese Academy of Sciences, China

<sup>4</sup>Harvard-Smithsonian Center for Astrophysics, 60 Garden Street, Cambridge, MA02138, USA

**Abstract.** We present a result of IRS spectroscopy of 14 Ultra-Luminous Infrared Galaxies (ULIRGs) in the Extended Groth Strip region. These galaxies are massive and have very high star formation rate. Four objects of this sample are detected in the *HST*/WFC3 near-infrared imaging. They show very diversified rest-frame optical morphologies, including string-like, extended/diffused, and even spiral with a possible bulge, implying different formation processes for these galaxies. We also search for signatures of active galactic nucleus (AGN) in our sample in the X-ray, mid-infrared and radio bands. This sample is dominated by objects with intensive star formation, only 14 – 29% of them have AGN activities.

**Keywords.** galaxies: fundamental parameters, galaxies: high-redshift, infrared: galaxies

---

## 1. Introduction

Ultraluminous infrared galaxies (ULIRGs) are defined by their characteristic infrared luminosity of more than  $10^{12} L_{\odot}$ , and were first discovered in the local Universe by *IRAS* (Sanders & Mirabel 1996). Although they contribute little to the infrared luminosity density in the local Universe due to small numbers, they become cosmologically important at  $z > 1$  (e.g. Le Floch *et al.* 2005). There are many ULIRGs detected at  $z \sim 2$ , including different types of objects, such as Submillimeter Galaxies (SMGs), MIPS 24  $\mu\text{m}$  selected ULIRGs, and Dusty Obscured Galaxies (DOGs) (Chapman *et al.* 2003; Houck *et al.* 2005; Huang *et al.* 2009).

Lots of works have been done for ULIRGs with  $L_{\text{IR}} > 10^{12.5} L_{\odot}$ . To investigate the relation between the redshift distribution, properties, and AGN fraction and infrared luminosity of ULIRGs, in this talk, we report a sample of ULIRGs with  $L_{\text{IR}}$  lower than those in previous studies.

## 2. Sample Selection and IRS Observations

In the redshift range  $1.4 < z < 2.7$ , the four IRAC bands probe the rest-frame NIR bands where galaxy SEDs have similar shape, thus the IRAC colors are very robust in determining their redshifts in this range where the 1.6  $\mu\text{m}$  bump shift into the IRAC bands. At  $z > 1.4$ , the 1.6  $\mu\text{m}$  bump moves in between the IRAC 4.5 and 5.8  $\mu\text{m}$  bands, thus  $[3.6] - [4.5] > 0$ . However, very dusty galaxies with a power-law continuum can have  $[3.6] - [4.5] > 0$ , even with redshift  $z < 1.4$ . To exclude those dusty galaxies/AGNs with power-law and also galaxies at  $z > 2.7$ , we propose an additional color cut of  $[5.8] - [8.0] < 0$ . Therefore, the color criteria for our faint 24  $\mu\text{m}$  sample for IRS spectroscopy are:

$$[3.6] - [4.5] > 0 \quad \& \quad [5.8] - [8.0] < 0. \quad (2.1)$$

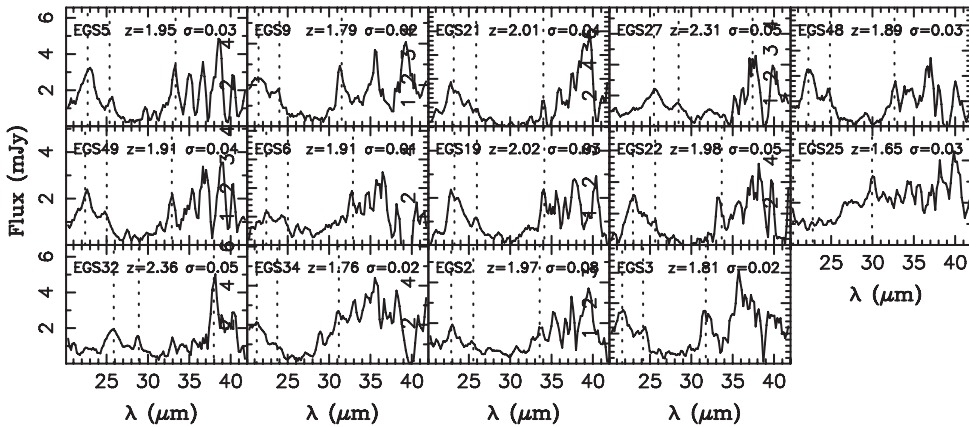


**Figure 1.** Mid-infrared spectra for 14 sources with redshift measurements. The dashed lines indicate the central wavelengths of the PAH emission features at rest-frame 7.7, 8.6, and 11.3  $\mu\text{m}$  from left to right. In each panel, the redshift and source ID are labeled at the top. The spectra were smoothed by a 4 pixel boxcar in order to enhance the broad features such as PAH emission and silicate absorption.

This color criterion set selects galaxies in the redshift range of  $1.4 \lesssim z \lesssim 2.7$ , within which their 7.7  $\mu\text{m}$  Polycyclic Aromatic Hydrocarbon (PAH) emission feature remains in the wavelength range covered by the IRS.

The IRS targets for this study were selected from the 24  $\mu\text{m}$  sample in the Extended Groth Strip (EGS) region. Huang *et al.* (2009) performed the IRS spectroscopy for a bright 24  $\mu\text{m}$  sample with  $F_{24 \mu\text{m}} > 0.6$  mJy in this field. Now we select a fainter 24  $\mu\text{m}$  sample with  $0.2 < F_{24 \mu\text{m}} < 0.6$  mJy at  $z \sim 2$ , 11 of 14 objects satisfying our criteria of Eq. (2.1), and 3 X-ray sources (EGS25, EGS27 and EGS34) with colors satisfying the criteria in Huang *et al.* (2009) for comparison.

IRS observation of our sample is a part of the GTO program for the *Spitzer*/IRAC instrument team (program ID: 30327). The objects were observed only with the IRS Long-Slit Low-Resolution first order (LL1) mode with the wavelength coverage of 20 – 38  $\mu\text{m}$ . All spectra were first processed with the *Spitzer* Science Center pipeline (version 13.0). Extraction of source spectra was done with both the SMART analysis package and our customized software (Huang *et al.* 2009). Figure 1 shows the IRS spectra of the 14 sources in our sample. All objects in the sample show PAH emission features at 7.7, 8.6, 11.3  $\mu\text{m}$  in their spectra, and some have silicate absorption at 9.7  $\mu\text{m}$ . We cross-correlate two local templates, M82 and Arp220, to the observed spectra to measure their redshifts. Both templates yield very similar redshifts with a typical difference of  $\Delta z = 0.02$ . The M82 template fits all spectra better. Our sample has a mean of  $\bar{z} = 1.95 \pm 0.19$ , and is in redshift range  $1.6 < z < 2.4$ . Three X-ray sources have generally similar spectra as the rest of the sample. EGS25 and EGS27 have weaker silicates absorption and higher continuum. EGS34, however, has weak silicates absorption and weak PAH emission.

### 3. Physical properties of ULIRGs at $z \sim 2$

#### 3.1. Total Infrared Luminosity, SFR and Stellar Mass

Infrared luminosity is an important measurement in characterizing ULIRGs at  $z \sim 2$ . ULIRGs with different  $L_{\text{IR}}$  ( $L_{8\mu\text{m}-1\text{mm}}$ ) may have gone through different formation processes. Direct measurement of  $L_{\text{IR}}$  requires far-infrared (FIR) photometry, but this is not

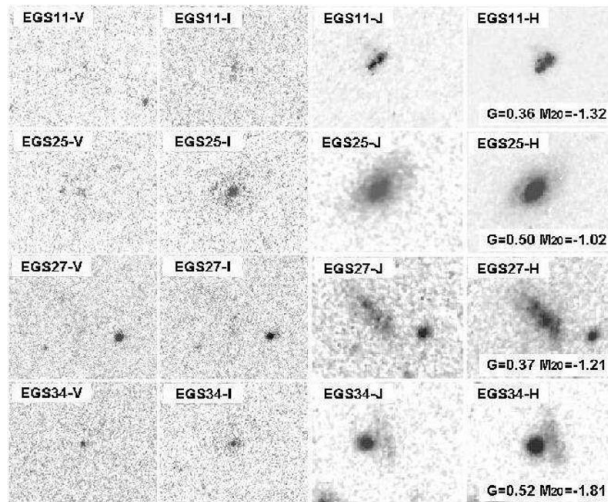


**Figure 2.** *HST*/ACS and WFC3 *V*–, *I*–, *J*–, and *H*–band images of 4 ULIRGs in the EGS (only four ULIRGs have both bands counterparts). Names and values of  $G$  (Gini coefficient) and  $M_{20}$  (the second-order moment of the brightest 20% of the light, Kong *et al.* 2009) are shown in each *H*–band image. All images are in negative grey scale and are  $6'' \times 6''$  in size.

available for most of  $24 \mu\text{m}$  selected sources. This is true for our sample. Many groups have made substantial efforts to convert MIR luminosities into  $L_{\text{IR}}$ . In this study, we use  $L_{\text{IR}} = 1.91(L_8 \mu\text{m})^{1.06}$  to calculate  $L_{\text{IR}}$  for our sample, which was confirmed with the *Herschel* SPIRE photometry (Caputi *et al.* 2007; Magdis *et al.* 2010).

All sources in our sample have  $L_{\text{IR}} > 10^{12} L_{\odot}$ . We converted the  $L_{\text{IR}}$  into SFR using the Kennicutt (1998) relation:  $\text{SFR} (M_{\odot} \text{ yr}^{-1}) = 4.5 \times 10^{-44} L_{\text{IR}} (\text{erg s}^{-1})$ . We derived a range of  $410 M_{\odot} \text{ yr}^{-1} < \text{SFR} < 1023 M_{\odot} \text{ yr}^{-1}$  for ULIRGs in our sample.

Using the Charlot & Bruzual (2007, CB07) models, spectroscopic redshifts of individual ULIRGs (from *Spitzer*/IRS), and their multi-wavelength spectral energy distributions (SEDs, from *U*-band to  $8 \mu\text{m}$ ), we have estimated the stellar-mass content for all ULIRGs in our sample. Daddi *et al.* (2007) suggested that the Kroupa IMF fits ULIRGs better. We fit the observed SEDs of each source using the CB07 stellar population models with a Kroupa IMF and a constant star formation rate. Stellar masses for objects in this sample are in the range  $10.9 < \lg(M_*/M_{\odot}) < 11.7$ .

### 3.2. Morphologies of ULIRGs

The Cosmic Assemblé Near-infrared Deep Extragalactic Legacy Survey (CANDELS) performed the largest *HST* F125W and F160W imaging survey with the newly installed NIR camera WFC3. Its high angular resolution permits the study of galaxy morphology at high redshifts (Grogin *et al.* 2011; Koekemoer *et al.* 2011). The EGS is one of the five fields in the CANDELS. Currently only a part of the CANDELS EGS imaging is available now, and 4 objects in our sample, EGS11, EGS25, EGS27, and EGS34, are detected in F125W and F160W. We compare their optical and NIR morphologies in Figure 2. These four objects are so red that they are barely detected in the F814W band. Their rest-frame optical morphologies are very diversified, including string-like, extended/diffused, and even early type spiral morphologies, implying that there may be different formation processes for these ULIRGs with different  $L_{\text{IR}}$ . It needs to be confirmed with a larger sample when the CANDELS imaging is complete.

### 3.3. AGN in ULIRGs

ULIRGs at  $z \sim 2$  can be divided into two types according to their IRS spectra, some of them with strong power-law continuum in mid-infrared are powered mainly by AGNs, while some others with strong PAH emission are powered by intense star formation.

We search for AGN signature in our sample using X-ray, radio, and MIR emission. Four objects (EGS22, EGS25, EGS27, and EGS34) out of 14 sources in the sample are detected in X-ray. The X-ray luminosities for EGS22 and EGS34 can be accounted for by their intense star formation. EGS25 and EGS27 have higher  $L_{2-10 \text{ keV}}$  than what their star formation can produce, indicating that they harbor an AGN. The MIR study of this sample with the 8 and 15  $\mu\text{m}$  photometry shows that 3 X-ray sources (EGS25, EGS27, and EGS34) have the highest 4.5  $\mu\text{m}$  luminosities and reddest [4.5] – [8.0] colors, consistent with them being AGN dominated. The FIR-radio ratios ( $q$ ) for this sample are very close to  $q = 2.35$  without showing strong radio excess from AGN, except EGS9 which has  $q = 1.66$ . Thus 14 – 29% of the sample show signatures of AGNs in X-ray, MIR or radio.

## 4. Summary

In this paper, we select a sample of 14 MIPS 24  $\mu\text{m}$  sources with  $0.2 < F_{24 \mu\text{m}} < 0.6$  mJy in the EGS region, with our new set of color criteria. These new color criteria can weed out the AGNs which would be included with the previous selection criteria. We have observed the mid-IR spectra of these galaxies with *Spitzer*/IRS. Using the PAH features at 7.7, 8.6, and 11.3  $\mu\text{m}$  in the IRS spectroscopy, we have measured the redshifts of our sample galaxies, and found the distribution of redshifts to be in a very narrow range,  $z \sim 1.95 \pm 0.19$ .

We fitted the multi-wavelength SEDs of the sample galaxies from the  $U$ -band to 8  $\mu\text{m}$ , and found they are massive galaxies, with a strong star formation activity. Four objects of this sample are detected in the *HST*/WFC3 NIR imaging. They show very diversified rest-frame optical morphologies, implying different formation processes for these galaxies. We also search for signatures of AGN in our sample in the X-ray, MIR and radio bands. This sample is dominated by objects with intense star formation, only 14 – 29% of them show AGN activity.

## Acknowledgements

This work is supported by the National Natural Science Foundation of China (No. 10873012) and Chinese Universities Scientific Fund (CUSF).

## References

- Caputi, K. I., Lagache, G., Yan, L., *et al.* 2007, *ApJ*, 660, 97
- Chapman, S. C., Blain, A. W., Ivison, R. J., *et al.* 2003, *Nature*, 422, 695
- Daddi, E., Dickinson, M., Morrison, G., *et al.* 2007a, *ApJ*, 670, 156
- Grogin, N. A., Kocevski, D. D., Faber, S. M., *et al.* 2011, *ApJS*, 197, 35
- Houck, J. R., Soifer, B. T., Weedman, D., *et al.* 2005, *ApJ*, 622, L105
- Huang, J.-S., Faber, S. M., Daddi, E., *et al.* 2009, *ApJ*, 700, 183
- Kennicutt, R. C., Jr. 1998, *ARAA*, 36, 189
- Koekemoer, A. M., Faber, S. M., Ferguson, H. C., *et al.* 2011, *ApJS*, 197, 36
- Kong, X., Fang, G. W., Arimoto, N., & Wang, M. 2009, *ApJ*, 702, 1458
- Le Floc'h, E., Papovich, C., Dole, H., *et al.* 2005, *ApJ*, 632, 169
- Magdis, G. E., Elbaz, D., Hwang, H. S., *et al.* 2010, *MNRAS*, 409, 22
- Sanders, D. B. & Mirabel, I. F. 1996, *ARAA*, 34, 749